INDIRECTLY DRIVEN, HIGH-CONVERGENCE IMPLOSIONS (HEP1)

S. P. Hatchett *S. M. Lane* *M. B. Nelson*

M. D. Cable *C. Laumann* *D. W. Phillion*

J. A. Caird *R. A. Lerche* *H. Powell*

J. D. Kilkenny *T. J. Murphy* *D. B. Ress*

H. N. Kornblum *J. Murray*

Introduction

High-gain inertial confinement fusion will most readily be achieved with hot-spot ignition,[1,2] in which a relatively small mass of gaseous fuel at the center of the target is heated to 5–10 keV, igniting a larger surrounding mass of approximately isobaric fuel at higher density but lower temperature. Existing lasers are too low in energy to achieve thermonuclear gain, but hydrodynamically equivalent implosions using these lasers can demonstrate that the important, scalable parameters of ignition capsules are scientifically and technologically achievable. The experiments described in this article used gas-filled glass shells driven by x rays produced in a surrounding cavity, or hohlraum. These implosions achieved convergence ratios (initial capsule radius / final fuel radius) high enough to fall in the range required for ignition-scale capsules, and they produced an imploded configuration (high-density glass with hot gas fill) that is equivalent to the hot-spot configuration of an ignition-scale capsule. Other recent laser-driven implosions[3,4] have achieved high shell density but at lower convergences and without a well defined hot spot. Still other experiments[5,6] have used very-low-density gas fill to reach high convergence with unshaped drive (see below), but that approach results in a relatively low shell density. Moreover, even at the highest convergence ratios the implosions described here had neutron yields averaging 8% of that calculated for an idealized, clean, spherically symmetric implosion—much higher than previous high-convergence experiments.

As we discuss below, the implosions described here were characterized by a number of diagnostics. In particular, convergence ratios were directly determined by measurements of the areal density of the imploded fuel using a technique based on secondary-neutron spectroscopy. The implosions were modeled, with the inclusion of non-ideal effects, with detailed computer codes such as LASNEX,[7] a coupled radiation transport, hydrodynamics, and burn-particle transport code. All observable quantities were in close agreement with these simulations, demonstrating good understanding of the implosions.

Experimental Design

The capsules, shown in Fig. 1, were indirectly driven gas-filled microballoons. We chose a relatively small capsule (capsule diameter 16% of hohlraum diameter) to limit the areal density of the imploded fuel, allowing the use of secondary neutrons for the determination of this quantity (see below). We used glass capsules filled with deuterium (D) or equimolar deuterium / tritium (DT). Capsule fill pressures varied from 25 to 200 atm, which changed the capsule convergence for constant drive (see "Measuring Convergence"). Ten Nova beams (2.1 kJ each at 0.35 μm) were incident on the interior of a uranium (U) hohlraum at 2×10^{15} W / cm^2 and produced an x-ray drive flux on the surface of the capsule; the hohlraum geometry is shown in Fig. 1(b). Figure 2 shows the measured laser power P_L, corresponding brightness temperature of the x-ray drive T_{rad}, and the neutron production rate R_n.

We measured x-ray drive using a multichannel, K- and L-edge–filtered x-ray spectrometer looking into the hohlraum at both directly illuminated laser spots and the indirectly illuminated wall;[8] observed spectra were nearly Planckian. Subject to hydrodynamic instability limitations,[9] we chose the x-ray drive vs time dependence, or pulse shape, to optimize the pressure–density trajectory of the capsule compression. Use of a glass shell and a U hohlraum minimizes the x-ray preheating of the capsule. The capsule implosion is driven by pressure generated by ablation of the outer surface material. Under the conditions of these experiments—x-ray brightness temperature low enough that the ablation front is subsonic, time-scale short enough that the ablated material is optically thin to the driving x rays—it can be shown[10] that the ablation pressure is

UCRL-LR-105821-95-4

approximately given by $P_{abl} = 0.5\sigma T_{rad}^4 / (RT_{rad}/\mu)^{1/2}$ where σ is the Stefan–Boltzmann constant, R is the gas constant and μ is the molecular weight. This gives ablation pressures of 8 Mbar at the foot of the pulse (t = 0.2 ns) and 110 Mbar at the peak of the pulse (t = 1.4 ns).

Achieving High Convergence

In implosions such as these, several factors limit the convergence ratio achievable. The most important are pusher entropy, drive asymmetry, and Rayleigh–Taylor (RT) instability. These factors must be minimized in the experiments and properly accounted for in models.

The first factor is pusher entropy. The less dense the pusher is near stagnation, the less efficiently it can couple its kinetic energy into compressing the fuel. X-ray preheat of the pusher raises its specific entropy; ablation pressure cannot then hold it at as high a density during inward acceleration, and at stagnation more of its kinetic energy will be spent compressing itself rather than compressing the fuel. X-ray preheat is minimized by the use of a U hohlraum, with the resulting near-Planckian x-ray spectrum, and a glass pusher, which self shields from hard x rays. Similarly, pulse-shaping is required to limit pusher entropy generation by shocks and to keep the pusher dense during inward acceleration. In the ideal, lowest entropy state, the pusher pressure results entirely from the Fermi degeneracy of the free electrons. In Figure 3, we plot the ratio of the pressure to the electron degeneracy pressure as a function

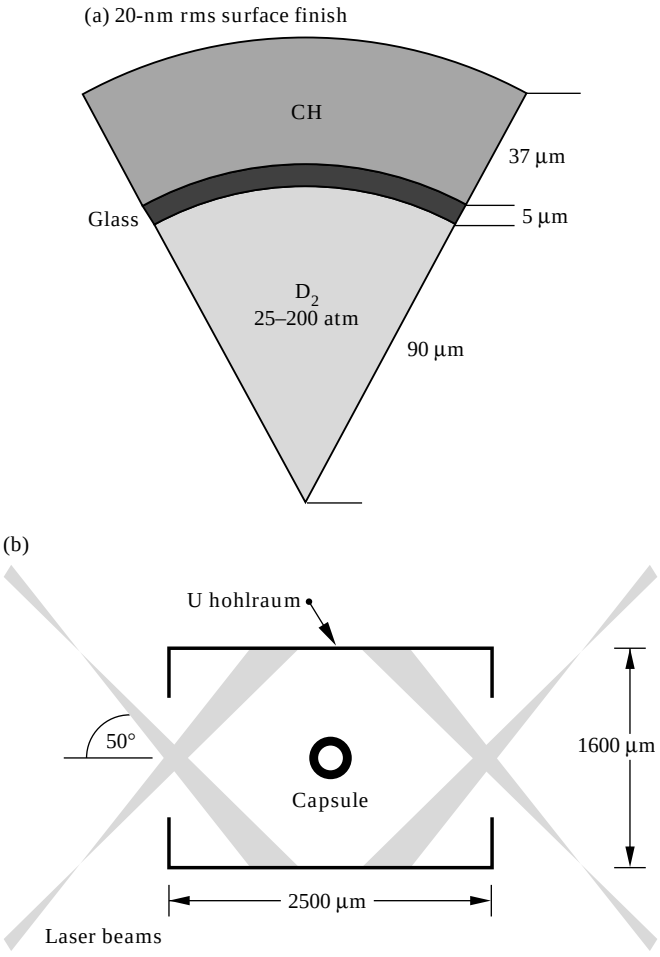

FIGURE 1. Capsule and indirect-drive hohlraum geometry. (50-05-0695-1562pb01)

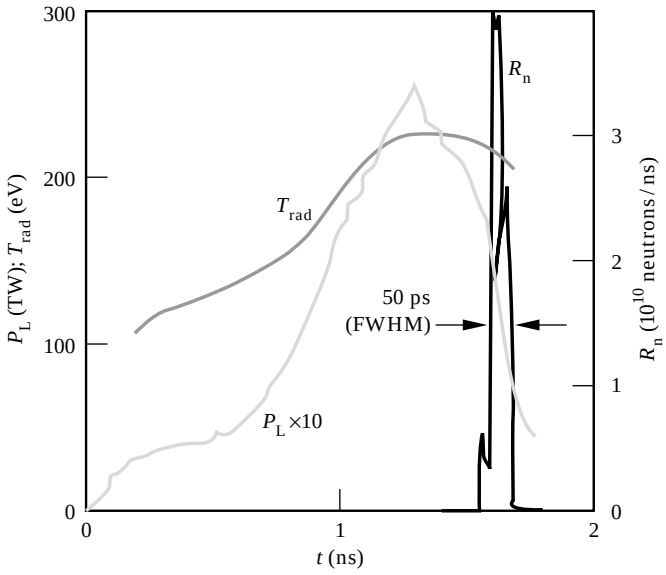

FIGURE 2. Observed laser power P_L, hohlraum temperature T_{rad}, and neutron production rate R_n for 100-atm DT-filled capsules. (50-05-0695-1563pb01)

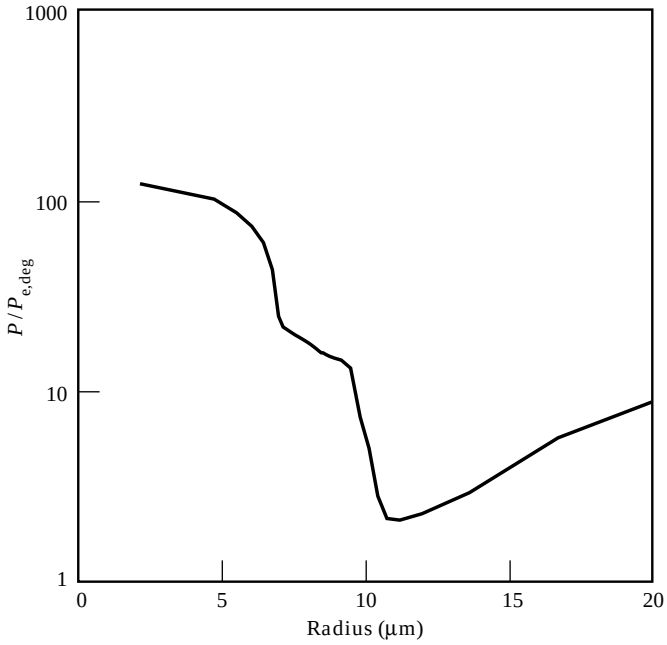

FIGURE 3. Ratio of pressure to electron degeneracy pressure in fuel and pusher of 100-atm fill capsules at bang time as calculated with the Haan mix model. The dense glass pusher, from 10 to 15 μm, is in a good, low-entropy state. (50-05-0695-1564pb01)

of radius through the fuel and pusher at the time of peak neutron production (*bang time*) in a model calculation of the implosion of a 100-atm DT-filled capsule. Figure 3 shows three more or less distinct regions: clean fuel (0–7 μm), mixed fuel and glass (7–10 μm), and dense glass pusher (10–15 μm). The pusher has been compressed along a good low-entropy $P(\rho)$ trajectory, or adiabat, so that its pressure is only a factor of about two above the Fermi degeneracy pressure. This capsule has the sort of compressed configuration—isobaric with a hot spot surrounded by colder and denser matter—described in the introduction for a high-gain capsule implosion.

X-ray drive asymmetry is the second factor limiting convergence. The hohlraum does not produce a perfectly uniform drive distribution, but any position on the capsule "sees" radiation from all the various elements of the hohlraum (directly illuminated wall regions, indirectly illuminated regions, and entrance holes), so higher moments of the drive distribution are strongly smoothed. (Typically the drive symmetry is analyzed in terms of spherical harmonics, which reduce to Legendre polynomials P_l with cylindrical symmetry.) The remaining systematic asymmetry is controlled by choosing the relative values of capsule radius, hohlraum dimensions, and the first bounce position of the laser beams along the hohlraum wall to minimize the P_2 and P_4 effects. P_1 and P_3 effects are eliminated by the left-right symmetry of the hohlraum. The remaining lower-moment asymmetry is time-dependent: both the albedo of the wall and the effective positions of the laser spots change as hot wall material moves into the hohlraum. By design with simulations, the configuration used in this work produces a P_2 asymmetry that changes sign, is at most 8%, and averages to a very low value. Details of hohlraum design are being reported in "Nova Symmetry: Experiments, Modeling, and Interpretation (HLP3 and HLP4)" on p. 293 of this *Quarterly*.

A second source of time-dependent drive asymmetry is random variations due to imprecise laser beam-to-beam power balance and pointing. This is minimized by precise control of the laser.[11,12] We maintain tolerances of 8% rms beam-to-beam power balance during the foot of the laser pulse and 4% power balance during the peak. Pointing tolerance is ±30 μm rms. This control gives a power balance on the capsule that from simulations is uniform to within 2% rms at peak power and 4% in the foot. Early experiments demonstrated that this level of power balance is necessary for high convergence. A version of Figure 6 with the early data showed convergence *declining* as fill was reduced.

Finally, since the fuel is compressed at stagnation by a denser pusher, convergence may be limited by RT instability at the fuel–pusher interface, which leads to what is commonly called *mix*. Calculations show that perturbations on the interface are primarily seeded by the feed-through of growing perturbations at the ablation front, which in turn are seeded by initial ablator surface finish perturbations. We have applied Haan's multimode, moderately nonlinear mix model[9] to calculations of the implosions of the 25- and 100-atm fill capsules. In this model, growth factors (final amplitude at fuel–pusher interface / initial amplitude at ablator surface) are calculated at a number of l-modes, initial amplitude $\propto P_l(\cos\theta)$, for perturbations small enough that the growth factors remain linear in the initial amplitudes. We then obtain an estimate of the rms depth of mix penetration by multiplying the initial surface-finish mode spectrum by the growth factors, applying a saturation model in which nearby modes contribute to the saturation of a particular mode, and then adding the saturated mode amplitudes in quadrature. There is an empirical parameter in the saturation model, which Haan calls ν, that must be estimated from mix experiments. (In the presence of a dense spectrum of modes, mode l has a saturation amplitude at radius R_0 of $\nu R_0 / l^2$.) Haan's current best estimate of this parameter is $\nu = 2$, which is the value we have used in our analysis.

Figure 4 shows the linear growth factors we calculated. At low l values (long wavelengths), the growth factors are comparable for the 25- and 100-atm capsules, whereas at higher l values the 100-atm capsules have much larger growth factors. This is a reflection of much more feed-through in the 100-atm case. When the first shock breaks out of the back of the glass pusher into the fuel, there is less decompression in the 100-atm case, leading to a thinner, denser pusher during inward acceleration. Were our pulse shape more highly

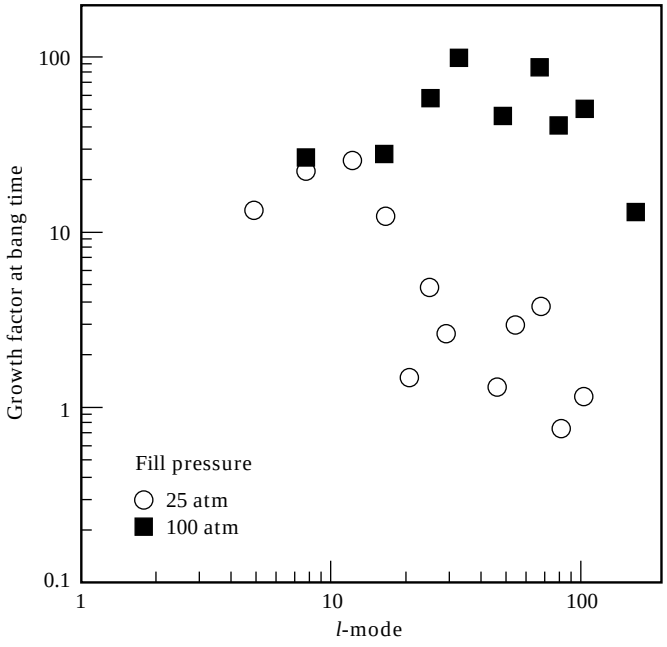

FIGURE 4. Calculated growth factors for surface perturbations on 25- and 100-atm fill capsules. (50-05-0695-1565pb01)

tuned, the 25-atm shells would have been thinner, but then mix and shell breakup might have destroyed their convergence altogether. As it is, with saturation applied, most of the quadrature sum of amplitudes at bang time comes from $l \leq 20$ for either fill pressure.

One way of expressing the depth of mix penetration is in terms of the distance from the fuel–pusher interface to the *fall line*, which is the trajectory the interface would have if it never decelerated at stagnation. For our capsules, the Haan model gives a bang-time mix depth—defined as the height of bubble tops above the interface—of about 35% of the distance to the fall line. Mix depth is not a constant with time, but rather it peaks at about that fraction near bang-time. Were it a constant, we would have another, simpler mix model, known as a *fracmix* model. In either model, the spike penetration—the distance from interface to spike tips—is estimated at $(1 + \alpha)$ times the bubble height, where α is the interface Atwood number.

Measuring Convergence

We determined burn-averaged fuel density and capsule convergence by measuring burn-averaged fuel areal density $\rho R \equiv \int_{\text{fuel}} \rho(r) dr$. If ρ is uniform, as we assume, then $\rho = \rho_0 (\rho R / \rho_0 R_0)^{3/2}$, so a determination of ρR gives both ρ and R. When we make comparisons later with calculations of ρ and R, we shall calculate those quantities in exactly the same way, with ρR determined from the calculated secondary neutron spectrum as described below for the experimental analysis. In fact, the uniform-ρ assumption gives a slight underestimate of the actual convergence and density because the actual density must increase with radius as the temperature decreases. From simulations, this is about a 15% effect in the density for the 25-atm capsules and about a 25% effect in the 100-atm capsules.

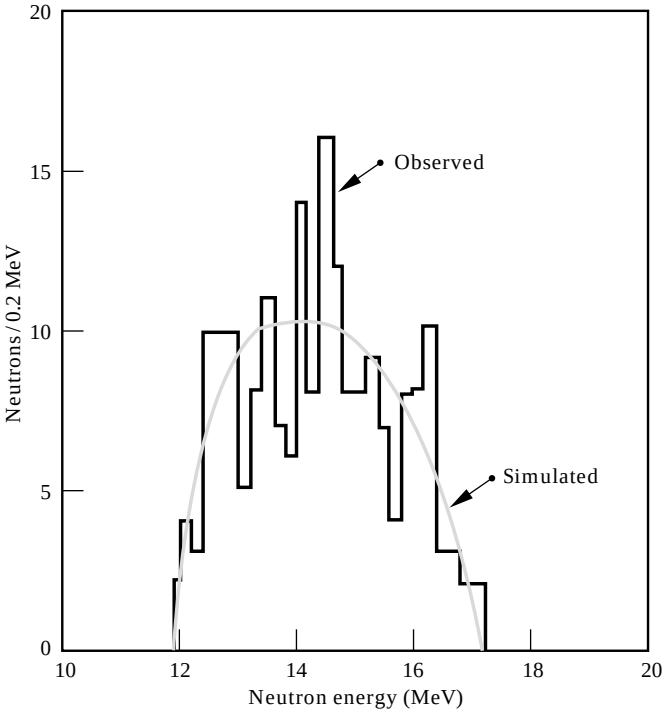

FIGURE 5. Secondary-neutron energy spectrum measured with array of neutron time-of-flight detectors (LaNSA). Observed is sum of spectra from all 25-atm capsules. (50-05-0695-1566pb01)

We measured fuel ρR by the secondary-neutron technique.[13–17] This technique relies on the observation of 12–17-MeV secondary neutrons produced via the D(T,n)^{4}He reaction in an initially pure D fuel. The 1.01-MeV tritium nuclei, or *tritons*, are produced in the primary fusion reaction D(D,p)T. If the tritons do not slow significantly as they traverse the fuel, then the fraction of tritons producing secondary neutrons is proportional to fuel ρR. For the fuel conditions in this work, (low temperature with mixed pusher material), ρR values above a few mg/cm^2 cause significant triton slowing, and corrections must be made for the energy dependence of the D(T,n)^{4}He cross section. Cable and Hatchett[13] have outlined how this can be done based on a measurement of the secondary-neutron energy spectrum. Since the cross section rises with decreasing triton energy, this correction typically results in a ρR value lower than that calculated for the case of little slowing. We measured the secondary-neutron energy spectrum with an array of neutron time-of-flight detectors (LaNSA).[18] Figure 5 shows a spectrum obtained by summing all the 25-atm capsule data; the figure also shows the spectrum obtained from calculations of these implosions with the Haan mix model, as discussed further below.

Observed fuel areal densities, which ranged up to 16 mg/cm^2, allowed us to determine the densities and convergences plotted in Fig. 6. For this figure, observed values were averaged over several implosions (two at 200 atm, six at 100 atm, and ten at 25 atm), and the errors were dominated by statistics related to the number of the observed secondary neutrons. Figure 6 shows that the observed values are consistent with or better than those expected from simulations if the effects of fuel–pusher mixing are included at the level that current models[9] predict given the capsules' surface finish. (The calculations labeled "clean 1-D" include no mix effects and assume perfect spherical symmetry; this is physically unrealistic but is commonly quoted as an "ideal" limit). Fuel–pusher mixing introduces two important effects: mixing of high-Z matter into the fuel enhances the triton slowing, and mixing of fuel outward into the pusher decreases the fuel convergence. Secondary-neutron spectroscopy allows us to quantify these effects since the secondary-neutron energy spectrum is dependent on the rate of the triton slowing. Figure 5 shows that the calculated and observed secondary spectra are in good agreement, which further supports the validity of the mix modeling.

Other Diagnostics and Discussion

We determined primary neutron yield[19] and pusher areal density[20] by activation techniques. We determined burn duration and burn time relative to the start of the laser pulse with a scintillator / streak camera arrangement[21] capable of measuring neutron production as a function of time with 20-ps resolution. Figure 2 shows an example of the measured reaction rate. We measured fuel ion temperature by observing the temperature-dependent Doppler broadening of the primary-neutron energy spectrum with a neutron time-of-flight system[22] that was simpler and separate from that used for secondary-neutron spectroscopy.

Primary-neutron yields for these implosions were 2×10^7 to 1.4×10^8 with pure D fill (2.45-MeV neutrons) and 3×10^8 to 3×10^9 with equimolar DT fill (14-MeV neutrons); the lower yields were observed for the higher-convergence, lower-fill capsules. Figure 7 shows the individual capsule yields and ρR values, with the yield expressed as a fraction of that calculated for a clean, 1-D implosion. Also shown for comparison are the values calculated for these implosions with the Haan mix model.

The scatter in ρR is consistent with the measurement error, but scatter in the yield is larger since yield is very sensitive to the fuel ion temperature (roughly

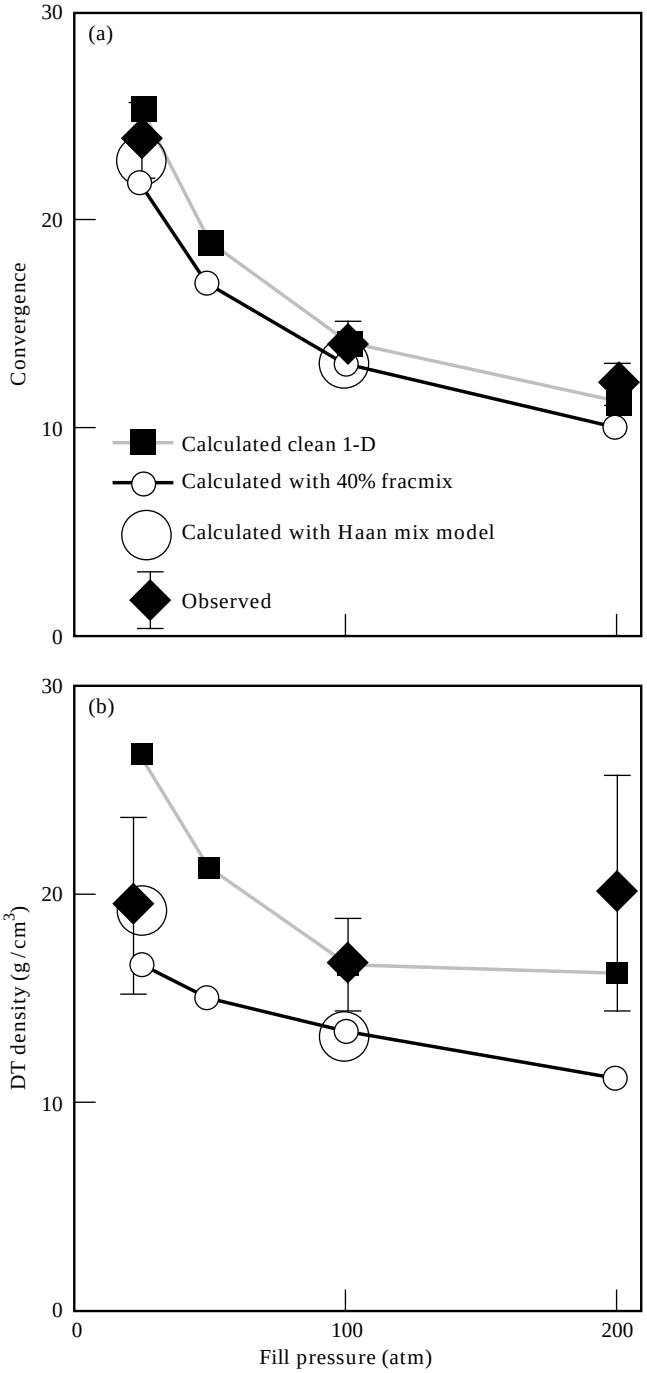

FIGURE 6. Observed and calculated (a) convergence and (b) density vs capsule fill pressure. Density is expressed as equivalent DT fill even when capsule is D-filled. (50-05-0695-1567pb01)

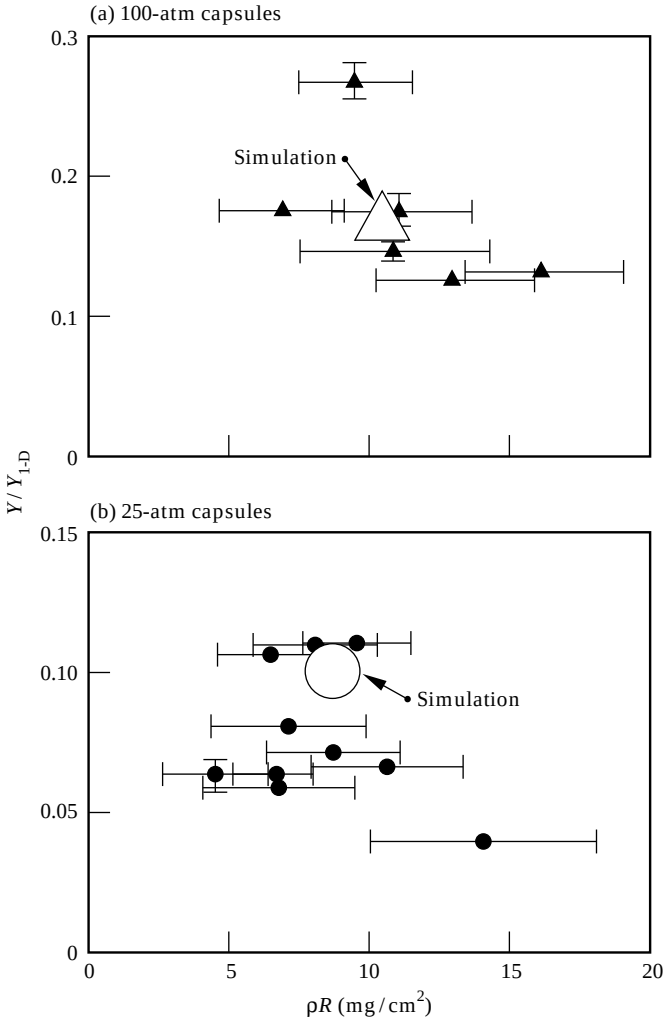

FIGURE 7. Observed neutron yields and ρR values for (a) 100-atm and (b) 25-atm capsules. Yields are plotted as a fraction of simulated clean 1-D yield. (50-05-0695-1568pb01)

proportional to T^5 for this temperature range) and because the fuel temperature is affected by small variations in capsule surface finish, capsule dimensions and laser energy. (The yield would be much less sensitive to mix if the glass pusher were replaced by a layer of cryogenic liquid DT, as it is in most current ignition-scale capsule designs.)

Fuel ion temperatures were 0.9 ± 0.4 keV for all cases; at this temperature, the observed fuel density corresponds to a final fuel pressure of 16 Gbar.

The glass shell ρR was 73 ± 16 mg/cm^2 (100 atm) and 60 ± 19 mg/cm^2 (25 atm) in a pair of shots at each fill. These values are about 1σ from the simulated values of 54 and 81 mg/cm, respectively. In the 25-atm simulations, the peak burn-time glass density is 160 g/cm^3.

Burn duration for the 100-atm capsules was 50 ± 15 ps; burn occurred at 1600 ± 100 ps after the start of the laser pulse (see Fig. 2); simulations gave 33-ps burn duration occurring at 1603 ps. We see in both simulations and measurements from a separate, brief experimental series that shock breakout, which corresponds to initial fuel movement, does not occur until 1 ns after the start of the laser pulse. This gives an average implosion velocity of 1.4×10^7 cm/s; simulations show that peak velocity is 1.8×10^7 cm/s. Using the observed fuel density and burn duration, we obtain a confinement parameter of $n\tau = 1.9 \pm 0.6 \times 10^{14}$ s/cm^3.

Summary and Conclusion

We have done a series of indirectly driven high-convergence implosions with the Nova laser fusion facility. These implosions were well characterized by a variety of measurements, and computer models are in good agreement with the measurements. We measured the imploded fuel areal density using a technique based on secondary-neutron spectroscopy. At capsule convergence ratios of 24, comparable to what is required for the hot spot of ignition-scale capsules, these capsules achieved fuel densities of 19 g/cm^3. Independent measurements of density, burn duration, and ion temperature gave $n\tau\theta = 1.7 \pm 0.9 \times 10^{14}$ keV-s/cm^3.

These experiments, which used better diagnostic techniques than previous work, have allowed detailed comparisons with simulations and have permitted a deeper understanding of the sensitivity of the implosion process to factors such as laser power balance. These implosions have provided an integrated test of our ability to control and model the implosion dynamics enough to achieve convergence ratios comparable to those required for the hot spot of an ignition-scale capsule.

Notes and References

1. J. Nuckolls, et al., *Nature* 239, 139 (1972).
2. J. D. Lindl, R. L. McCrory, and E. M. Campbell, *Physics Today* 45, 32 (1992).
3. F. J. Marshall, et al., *Phys. Rev. A* 40, 2547 (1989).
4. H. Azechi, et al., *Laser Part. Beams* 9, 193 (1991).
5. J. D. Kilkenny, et al., *Plasma Physics and Controlled Nuclear Fusion Research* (International Atomic Energy Agency, Vienna, 1989), vol. 3, p. 29.
6. H. Nishimura, et al., *Plasma Physics and Controlled Nuclear Fusion Research 1992* (IAEA, Vienna, 1993), vol. 3, p. 97.
7. G. B. Zimmerman and W. L. Kruer, *Comments Plasma Phys. Controlled Fusion* 11, 51 (1975).
8. H. N. Kornblum, R. L. Kauffman, and J. A. Smith, *Rev. Sci. Instrum.* 57, 2179 (1986).
9. S. Haan, *Phys. Rev. A* 39, 5812 (1989).
10. S. P. Hatchett, *Ablation Gas Dynamics of Low-Z Materials Illuminated by Soft X Rays*, Lawrence Livermore National Laboratory, Livermore, CA, UCRL-JC-108348 (1991).
11. J.A. Caird, R.B. Ehrlich, O.L. Landen, et al., *ICF Quarterly Report* 4(1), 10–17, Lawrence Livermore National Laboratory, Livermore, CA, UCRL-LR-105821-94-1 (1994).
12. J.E. Murray, M.C. Rushford, C.S. Vann, et al., *ICF Quarterly Report* 4(1), 18–24, Lawrence Livermore National Laboratory, Livermore, CA, UCRL-LR-105821-94-1 (1994).
13. M. D. Cable and S. P. Hatchett, *J. Appl. Phys.* 62, 2223 (1987).
14. E. G. Gamalii, et al., *JETP Lett.* 21, 70 (1975).
15. T. E. Blue and D. B. Harris, *Nucl. Sci. Eng.* 77, 463 (1981).
16. H. Azechi, et al., *Appl .Phys. Lett.* 49, 555 (1986).
17. M. D. Cable, et al., *Bull. Am. Phys. Soc.* 31, 1461 (1986).
18. M. B. Nelson and M. D. Cable, *Rev. Sci. Instrum.* 63, 4874 (1992).
19. S. M. Lane, et al., Lawrence Livermore National Laboratory, Livermore, CA, UCRL 50021-86 (1986).
20. S. M. Lane and M. B. Nelson, *Rev. Sci. Instrum.* 61, 3298 (1990).
21. R. A. Lerche, D. W. Phillion, and G. L. Tietbohl, in *Proceedings of SPIE 2002*, P. W. Roehrenbech, Ed. (San Diego, 1993), p. 153.
22. T. J. Murphy and R. A. Lerche, *Rev. Sci. Instrum.* 63, 4883 (1992).